

Report for Prototype of an Affordable Inserted Ventilator Tube Flow Meter

FERZEM KHAN,¹ ORION ARNDT,¹ AND JAY ZHANG (张翔宇)¹

¹*Department of Physics, University of Illinois at Urbana-Champaign, Urbana, IL, 61801, USA*

ABSTRACT

This paper describes prototypes for a ventilator flow meter based on Bernoulli’s principle, which can be used in a medical setting to monitor the gas flow between a shared split tube mechanical ventilator and an intubated patient. The design would facilitate sharing of a ventilator between several patients, each of whom are separately monitored using flow meters. The prototypes consists of a flow tube with pressure sensors connected to a printed circuit board via ribbon cables which is capable of data acquisition, local data storage on an SD card, data display on a thin film transistor screen, and transmission over a wireless network to a webpage or through radio to a base station. Various flow meter prototypes were tested for pressure sensitivity and performance stability, with the prototypes capable of measuring pressure differences over air flow rates of 5 to 25 litres per minute, with standard deviations ≤ 6 Pascals.

Keywords: Medical physics

1. INTRODUCTION

1.1. *Need for the device*

The Covid-19 pandemic brought about a critical scarcity of ventilator machines for patients in need of intubation in many countries, including the United States. This scarcity was far more serious in the developing world. For example, in early 2020 the Liberian Public Health Institute’s Director of the Infectious Diseases and Epidemiology Department stated that “there is just one ventilator in the country, located at a hospital outside of the capital” [1]. This shortage highlighted a glaring vulnerability in global healthcare infrastructure, which prompted a need for proactive measures to address such challenges to prepare for future pandemics, which affordable medical devices might help alleviate. The magnitude of the loss of life during the Covid-19 crisis made plain the need for inexpensive and easy to produce forms of medical care. While developing countries have needs for other forms of infrastructure, inexpensive medical devices like shared ventilator flow meters are designed to fill out lacking areas of healthcare in any system while detracting little from other needed resources like clean water or electricity in underdeveloped nations’ budgets.

Amidst the shortage of ventilators, a pragmatic solution which gained traction during the pandemic involved the shared use of a single ventilator among multiple patients. This approach is increasingly recognized as a feasible means of mitigating the scarcity of ventilators,

thereby saving more lives. In February 2021 the U.S. Food and Drug Administration posted a letter instructing proper use of ventilator splitters for healthcare facilities ([2]; also see [3]).

One limitation of this method when unmonitored is that it is functionally limited to two shared patients of very similar lung size, otherwise there is risk of lung damage to both patients due to over-filling the lungs. This is why implementation of effective, real-time air-flow monitoring is necessary for ventilator sharing to gain more widespread use. However, there exists a market vacuum for effective, affordable and convenient air-flow monitors for ventilator sharing. For example, the FDA’s “Emergency Authorized Use” list of accessories includes only one flow monitor, the “PEEP-Alert Pressure and Flow Monitor” which is not intended for intubation [2]. The PEEP (Positive end-expiratory pressure) Flow Monitor reports the pressure and flow rate averaged over three-second intervals with an accuracy of 10% - 15% depending on conditions, shows its readings on a display built into its case instead of uploading to a local server, and has a price of \$390 [4]. This highlights the market gap in intubated flow meters.

This spurred the development for an enhanced ventilator flow meter designed for intubation and accurate real-time monitoring based on Gollin’s prototype design [5]. This device features the capability to monitor airflow rates within ventilator tubes, with a Thin Film Transistor (TFT) screen providing real-time data

as well as graphs illustrating recent airflow rates. Furthermore, it can accurately timestamp and structure the data, which can be saved to a micro SD card connected to the TFT display. The user can also upload data to an online server via a private IP address using a wireless network (standard encryption, capable of Secure Sockets Layer encryption) [6] [7], integrating the data into hospital systems. The data is accessible through a simple web page for users on the wireless network. This ensures real-time, remote respiratory monitoring, which will enhance overall patient care. Unlike flow monitors available on the market, the prototype presented in this report has a comparatively lower estimated cost of \$120.

1.2. Physics Background

The behavior of fluids is well described by the continuity, Navier-Stokes, and Bernoulli’s equations as long as certain approximations are applicable. In this case, flow velocities are small compared to the speed of sound, while variations in pressure inside the device are at most a few percent of atmospheric pressure, so the tube can be divided into three parts where pressure is about the same inside each part before ventilation. Two parts are needed for the Bernoulli equation, and a third is useful for measuring the effects of fluid mechanics that do not fit the ideal fluid in Bernoulli’s equation. Therefore one can approximate two velocity-dependent pressures with the Bernoulli’s equation:

$$P_1 + \frac{\rho_1 u_1^2}{2} + \rho_1 g h_1 = P_2 + \frac{\rho_2 u_2^2}{2} + \rho_2 g h_2 \quad (1)$$

where g is earth’s surface gravitational constant, P is pressure, ρ is density, u is fluid velocity, and h is height; subscripts here refer to parameters in different parts of the tube, where pressure is approximately constant inside each part. Breath will have negligible affect on air density, so $\rho_1 \simeq \rho_2$. Assuming an ideal scenario where the flow is horizontal so that $h_1 = h_2$, the pressure difference is given by Equation 2.

$$P_1 - P_2 = \frac{\rho_1(u_2^2 - u_1^2)}{2} \quad (2)$$

To have a fluid flow of Q cubic meters per second through a tube with cross-sectional area A square meters requires a flow velocity (in meters per second) of

$$u = \frac{Q}{A} \quad (3)$$

An inspiratory flow rate of 30 liters/minute corresponds to $Q = 5 \times 10^{-4} \text{ m}^3/\text{s}$.

The airflow through the device is determined by measuring the pressure difference between the inlet and cen-

tral region of the flow tube with DPS310 pressure sensors. These are manufactured by Infineon Technologies AG and mounted onto small “breakout boards” by Adafruit Industries LLC.

1.3. Turbulent flow

Bernoulli’s equation applies to fluids undergoing laminar flow, but it doesn’t apply to fluids undergoing turbulent flow. The Reynolds number of the fluid and the channel it passes through can be used to determine whether a fluid might undergo turbulent flow. Systems with Reynolds number R_e less than 2,300 will usually exhibit laminar flow, while those with R_e greater than 2,900 will tend to show turbulence.

The Reynolds number for a tube is

$$R_e = \frac{u d_h}{\nu} \quad (4)$$

where u is the fluid’s velocity, d_h is the “hydraulic diameter” of the flow tube, and $\nu = 1.506 \times 10^{-5} \text{ m}^2/\text{s}$ is the “kinematic viscosity” of air at 20 °C. For a rectangular pipe that touches air on all its sides, $d_h = 4A/C$, where A is the cross-sectional area and C is the circumference or perimeter of the cross-section.

Combining Equations (3) and (4), the equation for a rectangular tube becomes:

$$R_e = \frac{4A}{C} \times \frac{Q}{A} \times \frac{1}{\nu} = \frac{4Q}{C\nu} \quad (5)$$

Equation (5) demonstrates that for a rectangular tube, the Reynolds number is proportional to Q , inversely proportional to perimeter C and ν , and independent of the cross-sectional area. This means that to decrease Reynolds number below the transitional threshold for a cross-section with fixed area, we need to increase its perimeter. The importance of this corollary will be discussed in Section 2.3.

2. PHYSICAL COMPONENTS

2.1. Circuit Board

The first prototype was a breadboard containing the minimum necessary hardware to record, display, and communicate data to another data storage device. It was designated to gather information and experience about how to use the component devices discussed later in Section 3. The size of the DPS310 and the o-rings meant the flow meter tube size could only mount the pressure sensors, necessitating a multi printed circuit board (PCB) system. A PCB was then created for the sensors that are mounted inside the flow meter tube (Figure 1), and a separate larger “home” PCB holds all other devices (Figure 2).

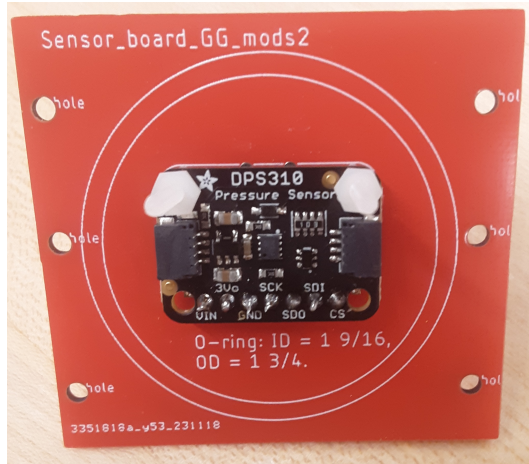


Figure 1. PCB Sensor Board.

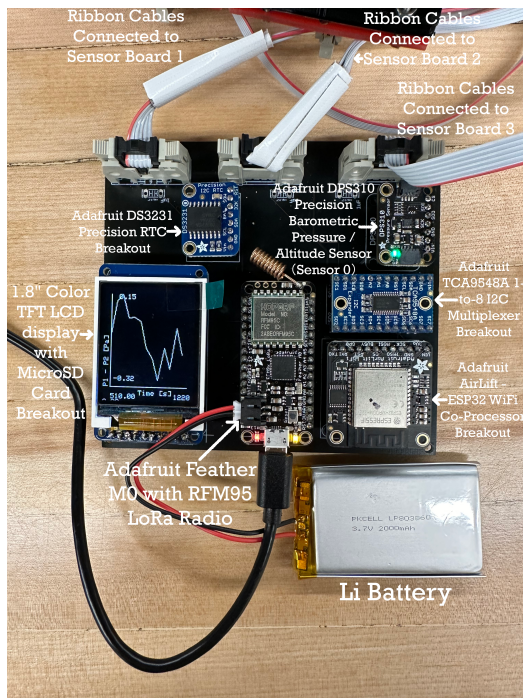


Figure 2. PCB Home Board.

2.2. Flowmeter Structure

The 3D printed structure (2 structures shown in Figure 3) is made from PLA (polylactic acid), a monomer made from fermented plant starch with a melting point between 130-180 °C. The box is made with one side as a separate lid to prevent issues with 3D printing hollow objects. The 3 sensors on 3 separate circuit boards will be exposed to the air flow via 3 large holes in the bottom of the flow meter structure. These will be sealed by EPDM o-rings, which will be pressured into sealing by 4 screws pressed into the screw holes of the sensor board

and structure. The lid is sealed with mounting putty or with super glue to avoid air leaks.

2.3. Attempts to Reduce Turbulence

There were multiple attempts to reduce turbulence of the device in order to ensure laminar flow, which necessitates reducing the Reynolds number Re . As Equation (5) shows, Re is proportional to Q , inversely proportional to C and v , and independent of the cross-sectional area. The first prototype had shown deviations from theoretical values calculated from Bernoulli's equation, suggesting turbulence. Therefore, flow meter tube geometries made for subsequent prototype designs have increased perimeter while keeping cross-sectional areas the same in order to reduce Re .

The prototypes had several other features that were designed to reduce turbulence as described in Table 1. Prototypes 2, 3, and 4 have fins attached to the lid to increase the surface perimeter in contact with the fluid. Prototypes 1, 3 and 4 have ramped wedges on the structure with the sensor boards (example in Figure 3) which would reduce sudden expansion of area present in the flow tube and hypothetically reduce turbulence.

3. HARDWARE

The main function of the device requires use of the DPS310 pressure sensor, manufactured by Infineon. The sensor has a accuracy and precision of 6 Pa and 0.2 Pa, respectively, for out of the box components. The accuracy is equivalent to the difference between pressures at a height difference of 60 cm at sea level. The precision is equivalent to the pressure difference for a height difference of 2 cm [8]. The devices are also temperature sensitive, with the device having a specific sensitivity of 0.5 Pa/K. The temperature sensitivity was tested for the intended operational range of the prototype (18 °C to 25 °C), with results discussed in Section 5.

Other devices which are utilized during this project are: the Radio Feather M0, the DS3231 clock, Adafruit Airlift Wifi, I2C multiplexer, Adafruit ST7735 TFT display, capacitors and ribbon head connectors (Figure 4).

- The RadioFeather is a processor chip, and all devices are directly or indirectly connected back to it. It is also capable of radio communication to a base station.
- The DS3231 RTC clock time stamps the data within the MicroSD card.
- The AirLift Wifi is necessary to send the prototype testing data to a retrievable storage device, and will be necessary in the final product to send

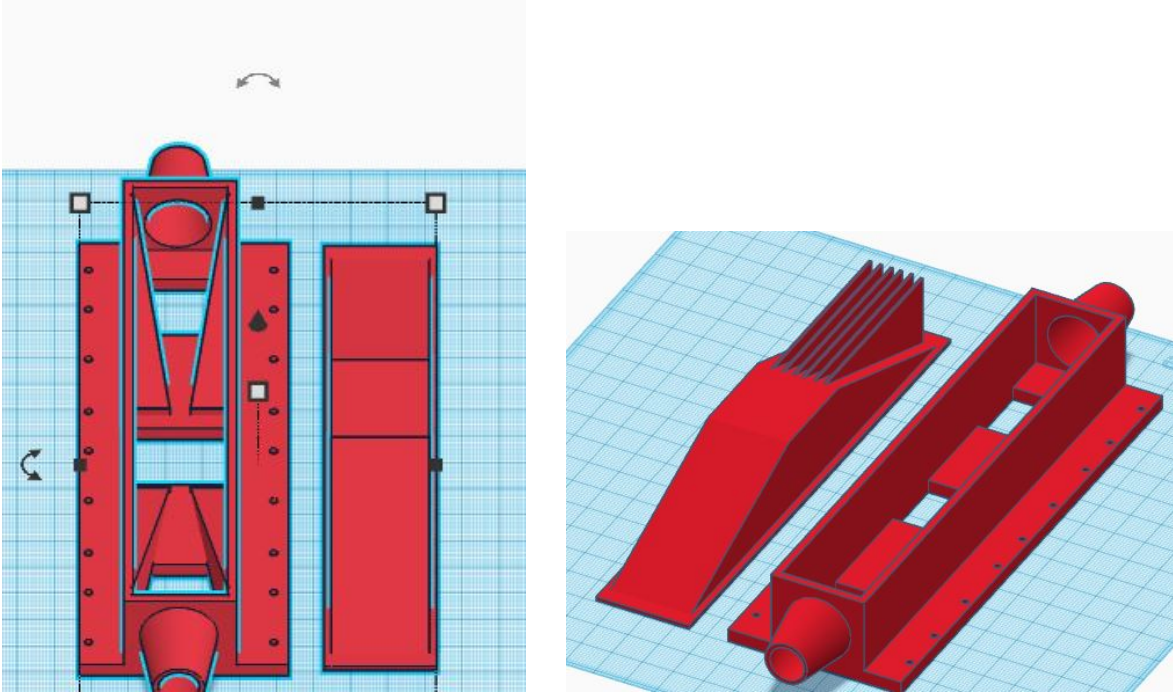


Figure 3. Prototype 1 (left) and 2 (right).

Prototype	Description	Cross-Sectional Area (Central Region) [mm ²]	Perimeter (Central Region) [mm]	Reynolds Number for Q=0.5L/s
1	Small cross-sectional area in the middle, tapering	12	16	8322
2	Anti-turbulence fins over the outlet sensor	20	42	3162
3	Same as 2 but with fins over middle sensor as well, tapering	69	52	2554
4	Same as 3 but with larger cross-sectional area	207	64	2075

Table 1. Different prototype geometries tested

information to the ventilator system within the hospital networks.

- The I2C multiplexer allows 4 or more sensors to send information to the radio feather. This would otherwise not be possible, as a feature of I2C devices is that multiple devices of the same part cannot be all plugged into the I2C ports. Each part shares I2C address unless made distinct by the multiplexer
- The TFT display allows an offline alternative for hospital staff to easily see the pressure and flow rates present in real time.

- The 1 μ F capacitors reduce power supply noise, which can slightly alter the reported measurements.
- The ribbon connectors are for the ribbon cables connected to the sensor boards so that they can flexibly be attached to the structure and the device can be more freely manipulated when attached to a flow tube.

4. SOFTWARE AND DATA ACQUISITION

Device functionality was programmed in the M0 using the Arduino Integrated Developers Environment (IDE), an open-source IDE with well documented and sup-

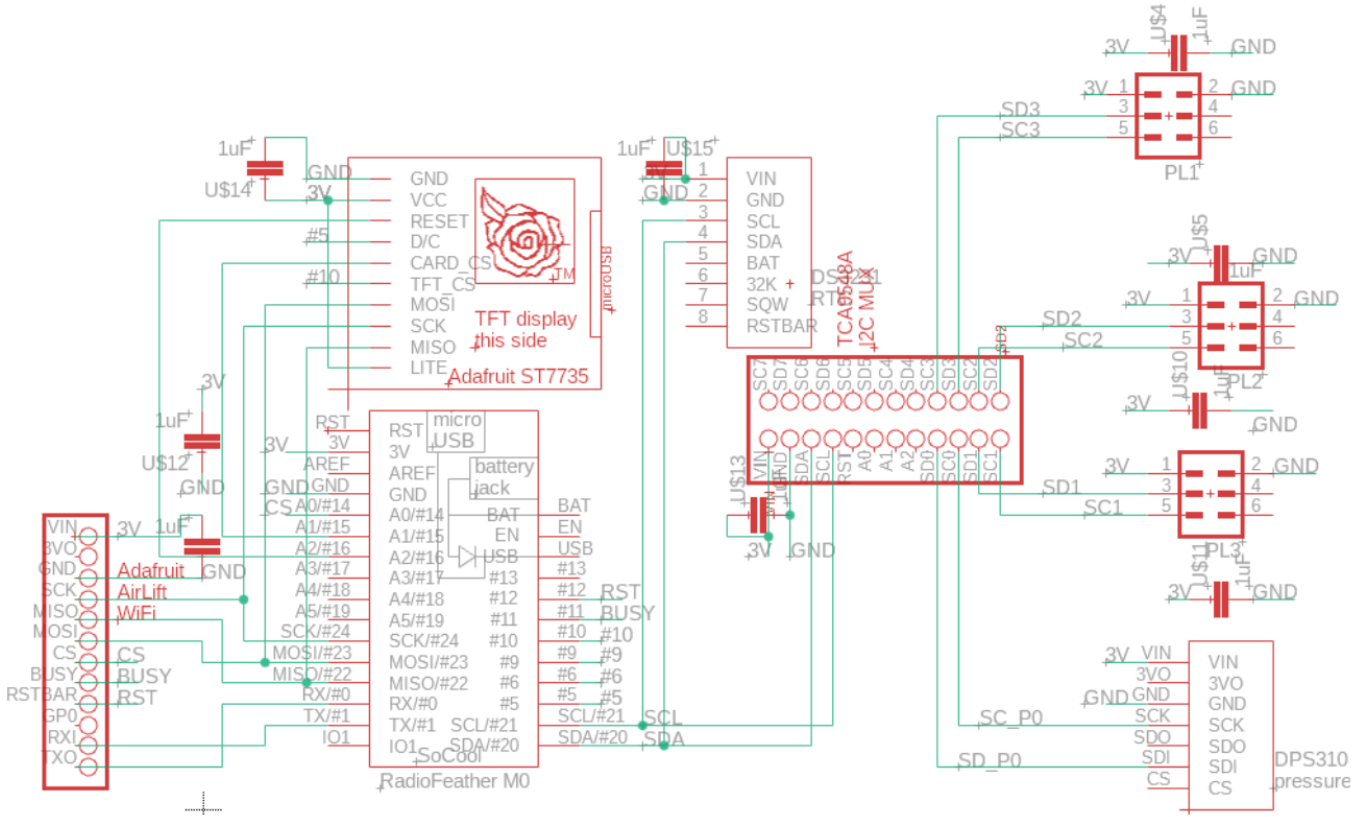


Figure 4. Home board schematic.

ported libraries for microprocessor communication, sensor detection, and wireless communication. For offline data analysis, the relevant code was written in Python. The main purpose of the Arduino IDE code is to set up the hardware, calibrate the DPS 310 sensors, read the data from sensors, perform local routines for storing data locally to an SD card and displaying data on the TFT display, and transmitting data over wireless communication. For wireless communication, which is the project priority for successful integration of the prototype in a medical setting, the data transmission capabilities offered by the WiFiNINA library were used, which can instantiate Servers, Clients and send/receive UDP packets through WiFi [6].

The data acquisition method is handled by the Arduino IDE code. The device takes some initial readings to calculate the mean pressure values and perform systematic corrections for the flowtube sensors with respect to the atmospheric pressure sensor. The prototype continuously takes readings and performs pressure corrections while the program is running. The frequency of the sensor reading is 1.02 Hz. The required readings are stored locally on an SD card and displayed on the TFT display. Since the readings are no more than 200 bytes per reading, a 16 GB microSD card will last a

few years at least, even with storing more data than the prototype is currently storing.

4.1. Data Transmission

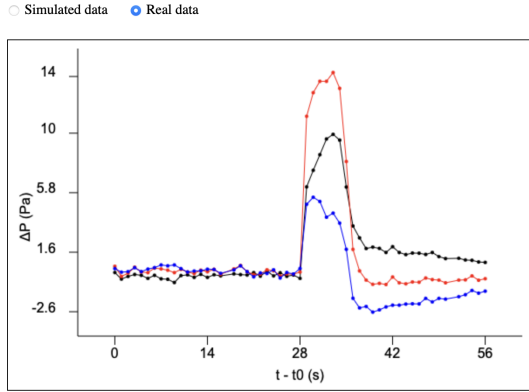
The prototype uses the IEEE 802.11 internet protocol to transmit data over a wireless network to a simple webpage that can be accessed over the campus network. The Airlift listens to client requests periodically (frequency of 1.5 – 2 seconds, taken to be a little more than the frequency of data collection) and sends back time, pressure and temperature readings for the individual sensors and the difference between P1 (inlet) and P2 (smaller cross-section). Currently, the web page shows the real time data recorded since the loading of the webpage on a local browser (Figure 5).

5. RESULTS

5.1. Calibration and Noise

The prototype performs pressure calibration in the setup to remove any biases and offsets from individual sensors by taking a set of initially 100 readings and calculating the mean and RMS of individual pressures and the pressure differences for all DPS 310 sensors. This would correspond to a roughly 100 seconds of "set-up" before the flow meter starts taking data, and this calibration time might need to be adjusted with regards to

Monitoring Pressures in the Ventilator Flowmeter



t0: Tue Apr 09 2024 16:35:38 GMT-0500 (Central Daylight Time)
 Black: P1 - P2, Red: P1 - P3, Blue: P2 - P3

Number of points: 55

Latest time: Tue Apr 09 2024 16:36:34 GMT-0500 (Central Daylight Time)

Pressures recorded by the 4 sensors (Pa):

98660.76
 98659.61
 98658.73
 98659.88

Figure 5. Screenshot of the webpage with real time data.

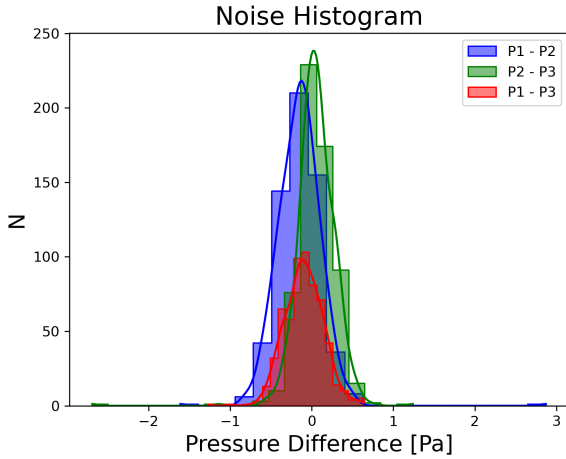


Figure 6. Histograms for noise between pressure sensors 1, 2, and 3.

medical demands (in case of emergencies for example). The program then calculates the corrected readings by subtracting the offsets between the individual sensors. Figure 6 shows the noise level DPS 310 sensors at the same height level, after correcting most baseline offsets. The noise histograms indicate a normal Gaussian distribution centered at 0 with a standard deviation within ± 0.25 Pa for the distribution.

5.2. Analysis

Prototypes with different geometries for a range of constant flow rates were tested. Considering the change

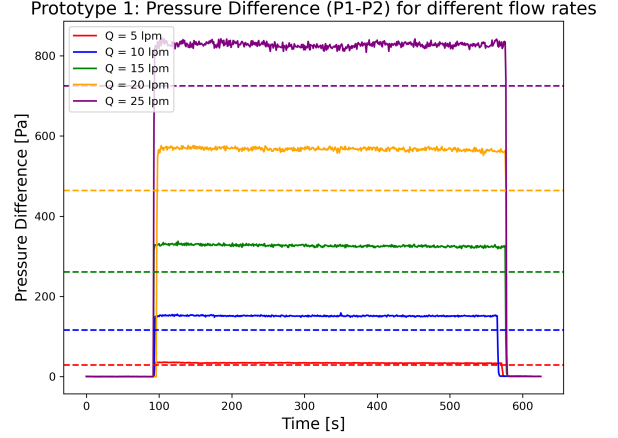


Figure 7. Pressure difference between the inlet and the middle region (P1 - P2) for different flow rates Q in Prototype 1. The dashed lines represent the theoretical pressure difference from Bernoulli's equation.

of kinematic viscosity within the range of room temperature ($18\text{ }^{\circ}\text{C}$ to $25\text{ }^{\circ}\text{C}$) to be negligible, a constant kinematic viscosity $\nu = 1.506 \times 10^{-5}$ m²/s at $20\text{ }^{\circ}\text{C}$ was assumed [9]. As expected, a smaller cross-sectional area of the central region resulted in a pressure difference between the inlet and the central region. Figure 7 depicts the pressure differences with time for one such prototype (Prototype 1) for different values of constant flow rates. The first ~ 100 readings are without any air flow in the flow meter tube, after which the air pump connected to the inlet that provides a constant flow rate was turned on. The device is stable for the duration of air flowing through the flow meter at a constant rate, with a standard deviation of 6.058 Pa at $Q = 25$ liters per minute.

The values of standard deviation of pressure difference (σ) are small for Prototypes 2, 3, and 4 (< 2 Pa) as compared to Prototype 1. Figure 8 depicts the mean pressure difference between the inlet and the middle section for different prototypes, fitted to a quadratic function using linear regression. The error bars in black represent 1σ values for the prototypes. The data seems to fit well to the quadratic polynomial ($Ax^2 + Bx + C$) between the pressure difference ΔP and volumetric flow rate Q , with R^2 values > 0.999 for Prototypes 1, 2 and 3, and $R^2 = 0.984$ for Prototype 4. The R^2 suggests that the data fits to a quadratic relationship between pressure difference and air velocity that isn't entirely represented by Bernoulli's equation.

From Bernoulli's equation, it is expected for the pressure difference between the central section (smaller cross-section) and the outlet (larger cross-section) of the

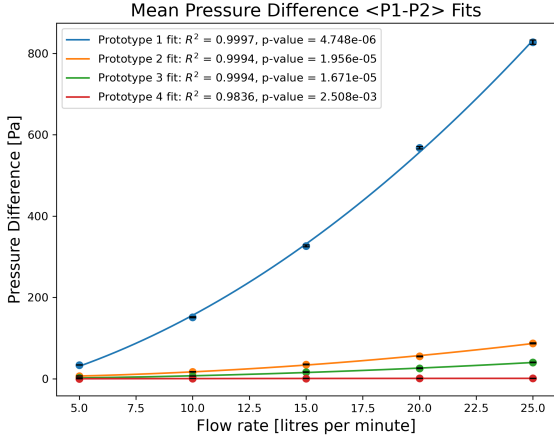


Figure 8. Mean pressure difference between the inlet and the middle region ($P_1 - P_2$) for different flow rates Q . Every color represents a different flow meter prototype, with each point giving the mean value and the lines representing the best fit curves to a quadratic function using linear regression.

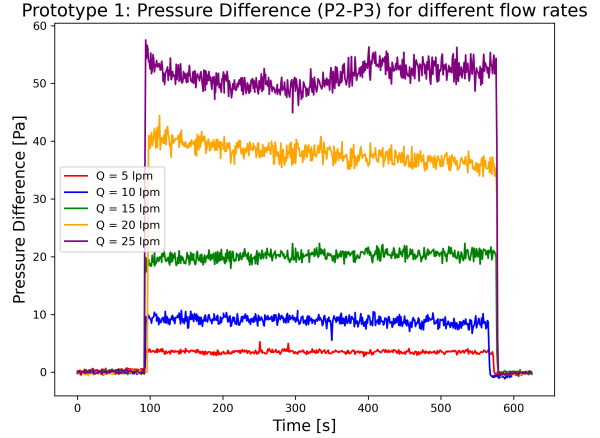


Figure 9. Pressure difference between the middle section and the outlet ($P_2 - P_3$) for different flow rates Q for prototype 1.

flow meter tube, ($P_2 - P_3$), to be negative and with a magnitude similar to ($P_1 - P_2$), since the outlet area has the same dimensions as the inlet area. However, the data presents positive values of ($P_2 - P_3$) across all flow meter prototypes and flow rates (Figure 9). This could be due to turbulence introduced in the flow meter’s central section, or due to energy loss due to dissipation. There were attempts to decrease turbulence in the device by using fins on top of the central and outlet sensors to streamline the flow, and by increasing the cross-sectional area of the central section. However, these attempts did not make a significant impact on the values of pressure difference ($P_2 - P_3$).

To check the stability of the device over a longer period of time, readings for over 40 hours were taken with no air flowing through the flow meter tube during that time. From the initial calibration of the pressure sensors, the pressure difference between sensors (initially 0 ± 1 Pa) drifted by $\sim 2 \pm 1$ Pa (Figure 10). These drifts seem to be characteristic of the physical position of the sensors and not the sensors themselves. The fluctuations are small compared to the magnitudes of fluctuations measured in Figure 7, indicating that the sensitivity of the device is not compromised. There might be a need to monitor this drift in a hospital setting in accordance with the accuracy desired by the medical personnel.

Over the intended operation temperature range for this device ($18 - 25^\circ\text{C}$), there was not an observed significant temperature dependence for pressure readings of our DPS 310 sensors. The coefficient of variation (of pressure difference with respect to time), defined as the value of standard deviation over the mean value,

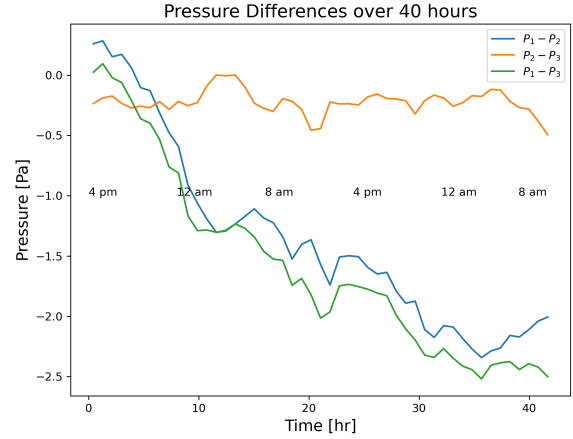


Figure 10. Pressure differences with respect to time taken over 40 hours with no air flowing through the flow meter tube.

($\sigma/\bar{\mu}$), is smallest for Prototype 1 (≤ 0.02), suggesting that the flow meter tube with specifications described by Prototype 1 is the most stable among the flow meter prototypes that have been tested.

6. CONCLUSIONS AND FUTURE WORK

The current prototype is able to successfully perform data acquisition using the I2C protocol from a flow meter tube with DPS 310 pressure sensors, and transmit data via radio or through wifi to a remote client (target personnel in a medical setting). The program successfully calibrates the DPS 310 sensors for pressure readings, and the flow tube design will be able to monitor the air flow in the flow meter for a patient for 5-25 liters per minute. The assumed standard for respiratory flow

rate is 30 liters per minute and ventilator systems can create higher flow rates. Thus the prototype needs to be extensively tested using respiratory simulation systems for higher flow rates to compare its performance to commercially available flow meters. Additionally, the pressure difference values are noticeably different from values assuming a laminar flow, which will affect flow

rate readings. Thus further testing and a better theoretical model that can account for turbulent flow is also needed for comparison to theory of fluid dynamics.

7. ACKNOWLEDGEMENT

We thank Professor George Gollin and Professor Yuk Tung Liu at University of Illinois for their technical support and guidance.

REFERENCES

- [1]Josh Holder. Tracking coronavirus vaccinations around the world. *The New York Times*, Mar 2023.
www.nytimes.com/interactive/2021/world/covid-vaccinations-tracker.html [Accessed 18 Apr. 2024].
- [2]Using ventilator splitters during the covid-19 pandemic. *FDA*, Feb 2021. <https://www.moph.gov.lb/userfiles/files/Medical%20Devices/Medical%20Devices%20Recalls%202021/10-02-2021/ventilatorsplittersduringthecovid19pandemic.pdf>.
- [3]Achanta et al. Development and evaluation of a mechanical ventilator-sharing system. *U.S. National Library of Medicine*, Feb 2024.
www.ncbi.nlm.nih.gov/pmc/articles/PMC10905385/ [Accessed 18 Apr. 2024].
- [4]Peep-alert pressure and flow monitor. *PEEP-Alert Technologies, Inc.*
web.archive.org/web/20231004162907/www.peep-alert.com/products/peep-alert [Archived 4 Oct. 2023. Accessed 18 Apr. 2024].
- [5]George Gollin. An inexpensive ventilator tube insertion flowmeter. Feb 2022. [unpublished].
- [6]Mistry et al. Wifinina library for arduino. *GitHub*.
github.com/arduino-libraries/WiFiNINA [Accessed 18 Apr. 2024].
- [7]Adafruit airlift – esp32 wifi co-processor breakout board. *Adafruit*. <https://www.adafruit.com/product/4201> [Accessed 18 Apr. 2024].
- [8]Dps310. *Infineon Technologies*, Oct 2020.
www.infineon.com/cms/en/product/sensor/pressure-sensors/pressure-sensors-for-iot/dps310/ [Accessed 13 Nov. 2023].
- [9]The relationship between the kinematic viscosity of air and temperature. *Cadence System Analysis*.
<https://resources.system-analysis.cadence.com/blog/msa2022-the-relationship-between-the-kinematic-viscosity-of-air-and->